International Journal of Fuzzy Logic and Intelligent Systems, vol. 3, no. 2, December 2003 pp. 178-186

Human Iris Recognition using Wavelet Transform and Neural Network

Seongwon Cho, Jaemin Kim, and Jungwoo Won

School of Electronics and Electrical Engineering, Hongik University

Abstract

Recently, many researchers have been interested in biometric systems such as fingerprint, handwriting, key-stroke patterns and human iris. From the viewpoint of reliability and robustness, iris recognition is the most attractive biometric system. Moreover, the iris recognition system is a comfortable biometric system, since the video image of an eye can be taken at a distance. In this paper, we discuss human iris recognition, which is based on accurate iris localization, robust feature extraction, and Neural Network classification.

The iris region is accurately localized in the eye image using a multiresolution active snake model. For the feature representation, the localized iris image is decomposed using wavelet transform based on dyadic Haar wavelet. Experimental results show the usefulness of wavelet transform in comparison to conventional Gabor transform. In addition, we present a new method for setting initial weight vectors in competitive learning. The proposed initialization method yields better accuracy than the conventional method.

Key words : iris recognition, active snake model, Haar wavelet, competitive leaning.

I. Introduction

Biometrics refers to the automatic authentification, identification, or verification of an individual based on physiological, behavioral and molecular characteristics. Research related to biometrics has developed rapidly in the last decades, and has led to various applications: security, smart card, and electronic commerce. Biometric techniques include recognizing faces, fingerprints, hands, iris, signatures, voices, DNA patterns, etc. Considering reliability and convenience, automated iris recognition is very attractive because human iris patterns are highly distinctive to an individual and the image of an eye can be taken at a distance [1].

The iris, visible through the clean cornea as the colored disc inside the eye, is a thin contractile diaphragm composed mostly of connective tissue and smooth muscle fiber. It lies between the cornea and the crystalline lens, and is attached to the eye's ciliary body and open to the pupil. The pupil lies approximately in the middle portion of the iris. The iris is composed of several layers: posterior surface, cooperative muscles, stromal layer, and anterior border layer. These multiplayer structures make the visual iris appearance. The anterior surface of the iris is divided into two basic regions: the central pupillary zone and the surrounding ciliary zone. The pupillary zone contains the sphincter muscle, and the ciliary zone contains the dilator muscle. The collarette, which forms the border between two areas and contains the minor arterial circle, appears as a zigzag circumferential ridge [2].

As the amount of light entering the eye diminishes in the dark, the iris dilator muscle runs radially through the iris and pulls away from the center. This muscle acts as one because individual cells bound together by connective tissues. When too much light enters the eye, the iris sphincter muscle, which encircles the pupil, pulls toward the center. These complex muscle movements cause the pupillary and ciliary zones to shrink or to expand and cause the zigzag pattern of the collarette to vary [2].

Various iris recognition methods have been proposed for automatic personal identification and verification. Daugman [4] first presented a prototype system for iris recognition. For the feature representation, it makes use of a decomposition derived from application of a two-dimensional Gabor filter to the iris image pattern. Quantized local phase angles yield the final representation. The similarity measure for feature classification is the Hamming distance between the acquired and data base representations. It reported excellent performance on a diverse database.

Wildes et al. [5] presented another iris recognition system. It decomposes the iris pattern into the multiresolution pyramid using a wavelet transform. Quantized differences between a level and its next lower resolution level yield the final representation. The similarity measure is the normalized correlation between the acquired and data base representations. It reported as good performance as the system of Daugman.

Both systems of Daugman and Wildes employ carefully designed image acquisition devices to get equal high quality iris images [5,6,7]. The devices minimize the deformation of the iris pattern due to the illumination variation, and acquire the sharp and glare-free iris images under fixed illumination. However, These demands are not easily satisfied in many field applications.

In this paper, we accurately localize the iris pattern using a multiresolution active snake model, efficiently extract features vector using Haar wavelet transform, and successfully classify extracted feature vectors using a neural net. This paper is organized as follows: In Section 2, we will review previous works. In Section 3, we will describe the iris acquisition

This work is supported in part by the Korea Sanhak Foundation

system used in our experiments. In Section 4, we will describe the accurate localization of the iris pattern by adapting the cost function of the snake model to the eye structure. In Section 5, we will describe how to extract compact feature vectors using Haar wavelet transform. In Section 6, we will describe how to learn LVQ with a new initialization and winner-selection method. Experiment results and discussion are shown in Section 7. Conclusion is shown in Section 8.

II. Previous works

Papers on the iris recognition are classified into four categories: image acquisition, preprocessing, feature extraction, and verification [4,5,6,7,8,9].

The image acquisition system consists of a simple lens, a monochrome CCD camera, and a frame grabbing board. A separate low-level tungsten halogen illuminator, an LED-based point light source, or infrared illuminators are used for the acquisition of a high-quality image of the iris. A beam splitter and a liquid crystal display are used to aid the user in alignment. To eliminate artifacts due to specular reflection, a polarizer is used [5,8].

Once an iris image is captured, the image is analyzed to locate the pupil and the limbus. The iris is between the limbus and the pupillary boundary. The iris pattern is represented by the image intensity value at the polar coordinate (r, θ), where r is the distance from the center of the pupil [4,5]. The localized iris pattern is then demodulated to extract features using a two-dimensional Gabor filter and the extracted complex-valued coefficients are encoded into 256 bytes codes or less [4,9]. The zero-crossing method based on one-dimensional wavelet transform is also used to extract features [6,7]. The normalized Hamming distance between a pair of iris codes or the normalized correlation is used for verification or identification [4,5,6,7].

III. IRIS Acquisition system

We make an iris acquisition system to automatically capture an iris image while remaining noninvasive to the human operator, which is shown in Fig. 1. When we take a photo of the iris pattern in a normal illumination condition, the photo is dark and does not have good contrast. To have good contrast in the interior iris pattern without annoying users, we use two infrared lamps, which consists of eight light-emitting diodes (LED). By careful positioning of the light source, the reflection of the source is placed inside the pupil. In this case, the major problem is reflections of the point source off eyeglasses. To eliminate these artifacts in the acquired images, we use directional infrared LEDs and adjust the directional angles of them. We puts an infrared-passing filter in front of the lens to eliminate reflection of various illuminant. To make iris images well framed without unduly constraining the operator, we put half mirror in front of the camera. Users can see what the camera is capturing and adjust his position accordingly. The captured image size is 320×240.

IV. Iris localization

For the localization of the iris pattern, we detect the inner boundary of the iris pattern, the pupillary boundary and the outer boundary, the limbus. Traditionally, the pupillary boundary and the limbus are modeled by two circles [4,5,9]. However, some pupillary boundaries are not equidistance from the center. In some cases, the inner and the outer boundaries are similar to ellipsis especially when the camera angle is not aligned to the normal direction of the eye surface. Accurate estimation of the inner and the outer boundaries is very important because features extracted from the iris pattern using a wavelet transform can be sensitive to this estimation error. In this section, we will explain a new method for accurate iris localization based on a multiresolution active contour model.

4.1 Active Snake Model for the Estimation of the Pupillary Boundary

Active contour models, called snakes, have been used for the estimation of object boundary [10,11]. We apply the well-known active contour model to the estimation of the inner boundary of the human iris. For the real-time implementation of the active contour model, we adopt Greedy algorithm proposed by Williams and Shah [11]. In the active contour model, the object boundary is represented by a sequence of nodes [illegible] of which the positions are determined by minimizing the global energy function. The global energy function is defined as follows:

$$E = \sum_{i=0}^{n} \left[\alpha E_{cont}(v(s_i)) + \beta E_{curv}(v(s_i)) + \gamma E_{image}(v(s_i)) \right], \quad (1)$$

where [illegible] is the continuity energy, [illegible] is the curvature energy, and [illegible] is the intensity energy. We adapt these energy functions to the characteristics of the human pupil. As for the continuity energy, we use the function proposed by Williams and Shah, which is defined as

$$E_{cont}(v(s_i)) = \left\| \bar{d} - \left| v(s_i) - v(s_{i-1}) \right| \right\|^2 \quad (2)$$

where $\bar{d}$ is the average distance between two nodes. As for the curvature function, we make the curvature at each node as close as possible to that of the circle as follow:

$$E_{curv}(v(s_i)) = \left\| \vec{v}_i - \left(\vec{u}(s_i)/|\vec{u}(s_i)| - \vec{u}(s_{i+1})/|\vec{u}(s_{i+1})| \right) \right\|^2, \quad (3)$$

where [illegible] is the curvature at the node and [illegible] is the curvature of the ideal circle at the node. For the computation of the intensity energy, we take the

gradient of pixel intensity in the radial direction at each node and integrate it along the arc as follow:

$$E_{image}(v(s_i)) = \int_{\theta_{i-1}}^{\theta_{i+1}} I(r,\theta) - I(r+\Delta r,\theta)d\theta, \quad (4)$$

where is the radius of the boundary.

4.2. Multi-resolution Active Snake

Greedy algorithm tends to converge to a local minimum, especially when the initialized node position has some error and noises are strong. In a fine resolution eye image, the initialization is relatively large error and the noise (due to long eyelashes and a thick eyelid) is strong. As a result, in 320×240 eye image, Greedy algorithm results in poor performance. This problem can be reduced by using a multiresolution method. Gaussian pyramids of the image are built and Greedy algorithm is performed starting from the lowest resolution level. At the lowest resolution level, the initialization error of each node is relatively small. However, this error can be still problem. To find an appropriate initial position of each node at the lowest resolution level, we use the characteristics of our image acquisition system with a special infrared illuminator. The reflection of the infrared illuminator is placed inside the pupil with a specific pattern. We detect the pattern using template matching and find the approximate location of the pupil in the acquired eye image. Using the information about the location of the pupil, we determine the initial position of each node. At the lowest level, the algorithm converges to the global minimum in a few iterations. In finer resolution levels, we progressively increase the number of nodes and reduce the search area. Fig. 9 (a)-(d) show the estimation results.

4.3 Estimation of the Limbus

In many cases, the limbus does not have sharp intensity transition, compared with the eyelid and eyelashes. Someone has a vague outline at the limbus. As a result, we have difficulty in detecting the limbus using the active snake model. When the camera angle is not aligned to the normal direction of the eye surface, the shape of the limbus is similar to an ellipse. We detect the limbus by estimating the distance from the center to the right boundary of the limbus, the distance from the center to the left boundary of the limbus, and the distance from the center to the bottom boundary of the limbus.

In each direction, we find the distance from the center to the limbus by minimizing the objective cost, which takes the gradient of pixel intensity in the radial direction at each node and integrate it along the arc as follow:

$$\min \int_{\theta_{i-1}}^{\theta_{i+1}} I(r,\theta) - I(r+\Delta r,\theta)d\theta. \quad (5)$$

When the limbus has a vague outline, the objective cost can be minimized inside the ciliary zone of the iris. To solve this problem, we use a multi resolution method, in which we find the approximate location of the limbus at the lowest resolution and progressively find the exact location of the limbus in a small search area. Fig. 9 (e)-(h) show the estimation results.

V. Feature extraction

For the extraction of features from the iris pattern, Gabor transform has been widely used[4,9]. Recently wavelet transform is also used [5]. In this section, we explain a new method for extracting feature from the iris pattern using a Haar wavelet transform. We use Haar wavelet because it can be implemented easily.

In this subsection, we briefly review a pyramid decomposition method [12]. To decompose a full-band one-dimensional signal into two subbands: L (low frequency band) and H (high frequency band), a low-pass filter acts on the signal and the filtered signal is down sampled, which generates L subband, and a high-pass filter acts on the signal and the filtered signal is down sampled, which generates H subband. By using this decomposition in the horizontal direction and in the vertical direction, a full-band two-dimensional signal is then decomposed into four bands: LL, LH, HL, and HH, where LH denotes one subband with horizontally low and vertical high frequency subband. This is shown in Fig. 2. For the pyramid decomposition, LL1 subband is decomposed into four bands: LL2, LH2, HL2, HH2. LL subbands are decomposed subsequently. This is shown in Fig. 3. The digital lowpass and high pass filters corresponding to Haar wavelet is [1,1] and [-1,1], respectively.

To analyze the iris image using two filter bank, the image, , in the polar coordinate is first transformed into the image, , in 2D Cartesian coordinate and then is decomposed into multiple subbands by the pyramid decomposition algorithm. Since sharp transition in the 2D iris pattern is well represented by each HH subband, we can use each pixel intensity values of a HH subband as the feature vector for the classification. Since HH1 subband has too many pixels and is sensitive to noises such as iris localization error or iris pattern variation due to the change in the intensity of illumination, we use a coarser HH subband such as HH3 or HH4. As the HH subband becomes coarser, the band becomes robust to the localization error but has less information.

To select the best HH subband to be used, we examined how successfully different iris patterns can be classified with a single HH subband. Fig. 4 and Fig 5 show the corresponding rates between the feature vectors. Fig. 4 uses HH4 and Fig. 5 uses HH5. In Fig. 4-5, black dots represent the corresponding rate between feature vectors of the same person and white dots represent the corresponding rate between feature vectors of different persons. In Fig 4, we can find the decision boundary (such as 65% corresponding rate) that classifies the iris pattern of one person from the others. In Fig. 5, we cannot find any decision boundary. This means that HH5 band does not have information enough to classify the iris pattern. Therefore, we extract most feature vectors from HH4 subband, which has $28\times3=84$ elements. Each element of the features are

quantized to two bits using a Lloyd-Max quantization without much degradation of performance. Finally, the feature vectors consist of 168 bits. This size is so small that the feature vector can be efficiently stored and processed.

VI. Neural network with uniformly distributed initial weight vectors

We classify the extracted feature vectors using a neural network. We learn the neural network with LVQ.

6.1 Initialization of Weighting Vectors

LVQ, a competitive learning method, is faster in a learning speed than the error back-propagation algorithm, but the learning speed and classification performance are sensitive to the initial weighting vectors. The simple method of initializing the weight vectors is to take the first m training vectors and use them as weight vectors; the remaining vectors are then used for training. Sometimes, weighing vectors are initialized to randomly selected training input vectors or the mean of the training vectors of each class. Other possible method of initializing the weights is to use K-mean clustering or CNN (condensed nearest neighbor) [13,14].

In LVQ, an appropriate initial weighing vector improves the learning time and classification performance. However, the distribution of initial weighting vectors chosen by initialization methods does not have large difference from the distribution of the training vectors. This is good for vector quantization but is not appropriate for a pattern classifier based on a Nearest Neighbor method. When a nearest neighbor classifier is used, an input vector is classified to the class represented by the weighting vector closest to it. Therefore, when we classify an input vector using reference (weighting) vectors with uniform distribution, only reference (weighting) vector close to decision boundaries between classes give contribution to the classification performance. Accordingly, we can improve the performance of LVQ by generating weighting vectors close to decision boundaries and by removing unnecessary weighting vector.

Based on this fact, we propose a uniform distribution initialization of weighting vectors, a new weight initialization method for competitive learning neural net, which generates the weighting vectors close to decision boundaries. The proposed method is as follows:

[Step 1] Among training vectors of each class, take the first input vector and use it as a weight vector for the class. The values of weighting vectors for the other classes are set to zero.

$$W_1^k = X_1^k \quad \text{for } k = 1, 2, \ldots, K$$

X_1^k : the first input training pattern of the k-th class

W_1^k : the first weighting vector for the k-th class

K : the number of classes

This is shown in Fig. 6.

[Step 2] For each class, feed an input vector into the network.

[Step 3] Compute the distances between input vectors and weighting vectors.

$$d(k,j) = \sum_{i=0}^{N-1} \left(X_i - W_{i,j}^k\right)^2 \tag{6}$$

X_i^k : the i-th element of the input vector

$W_{i,j}^k$: the i-th element of the j-th weighting for the k-th class

N : the dimension of the input vector

[Step 4] Determine whether the class represented by the weighting vector closest to an input vector is equal to the class of the input vector. Only if two classes are not equal, we take the input vector and use it as a new weighting vector, which is added to the network.

[Step 5] Do Step 2-5 until all training input vectors are processed. When all training input vectors are processed, some output neuron can have many weighting vectors as shown in Fig. 7.

When the data has widely scattered distribution, this method can make the number of neuron large and may not have good performance.

6.2 Dimensional Winner-Selection Method

As a distance measure, Euclidean distance is used in LVQ. However, when the dimension of the input vector is large, winner selection based on Euclidean distance can be wrong because of loss of information about each dimension of the input vector. We propose a new winner selection method based on a new distance measure. For each training input vector, we do the following steps:

[Step 1] Compute the distance from the first element of the input vector to the first element of each weighting vector.

[Step 2] Find the weighing vector of which the first element is closest to the first element of the input vector and increase the winning count for the weighting vector by one.

[Step 3] Do Step 1-2 until all elements of the input vector are processed.

[Step 4] After all elements are processed, the weighting vector with the largest winning count is the winner. Once the winning weighting vector is determined, we update the weighting vectors using a known LVQ updating method.

In determining the winner, the proposed dimensional winner-selection method can consider information about each element of the input vector (such as quality), and it takes a smaller computation time than a winner-selection method using other distance measures.

VII. Experiment Results

We use a database of 200 iris photographs: The photographs were taken from 20 peoples in different hours and days. We used 100 iris photographs for learning and 100 for test. The parameter values for LVQ are shown in Table 1.

7.1 Iris Localization

Fig. 2 shows the pupillary boundary and the limbus detected by the proposed method. The proposed method successively found the exact location of the inner and the outer boundaries of the iris in all 200 photos. The number of resolution levels is three.

7.2 Feature Extraction

We compared two different feature extraction methods based on Gabor transform and Wavelet transform. We used the same LVQ for two methods. The performance of two methods is shown in Table 2. As for the learning data, two methods result in the same performance. As for the test data, feature extraction based on wavelet transform results in slightly better performance.

7.3 Initialization of Weighting Vectors

We compared classification performance of two methods: one based on the proposed initialization method and the other based on a random initialization method. We used wavelet transform for feature extraction. The performance of two methods is shown in Table 3. The proposed initialization method results in better performance.

7.4 Winner Selection

We compared the proposed winner-selection methods and other ones. We used wavelet transform for feature extraction and the proposed initialization methods for the initialization of LVQ. 2-D Euclidean norm is generally used as a distance measure in LVQ but it does not guarantee better performance than other norms. For improving classification performance, we tested various norms. However, other norms do not improve the performance, which is shown in Table 4.

To figure out the effect of each elements of the input vector on the classification performance, we computed classification success rate in each dimension of the input vector. This is shown in Fig. 8. If all elements have the similar contribution to the classification performance, we can use Euclidean distance as a distance measure. However, most elements have more than 90% accuracy in the classification success rate, and some elements have less than 85% accuracy in classification success rate. This means that the proposed dimensional-winner selection method results in better performance than the winner-selection method based on Euclidean norm, which is shown in Table 5. In the proposed winner-selection method, we successfully classified all test data even when we use only 10 elements of the input vector with the highest classification success rate. This means that the proposed method is computationally effective.

7.5 The Size of Feature Vector

In the subsection 7.2~7.4, we experimentally showed that the proposed methods resulted in better classification performance. In the subsection 7.4, we showed that the proposed winner-selection methods could reduce the dimension of the feature vector. In this subsection, we compared the proposed methods with a small feature size, 84 dimensions (2 bit per a dimension) and other method with a relatively large feature size, 93 dimensions (4 bytes per a dimension) [15]. Table 8 shows that the proposed method with smaller feature size results in as good performance as the method with larger feature size. We summarize the results of four experiments in Table 9. The execution time for iris recognition takes less than 1 seconds on Pentium III (1.0GHz, 256MB RAM).

VIII. Conclusion

In this paper, we have described the iris recognition system with high classification success rate. For the accurate localization of the iris pattern, we used a multiresolution active snake model, in which each components of the energy function is adapted to the characteristics of the human eye. For the feature extraction, we used dyadic Haar wavelet transform, which is experimentally shown to be better than Gabor transform in classification performance. To improve classification rate, we used a neural network based on LVQ. For the learning of LVQ for the iris recognition, we proposed a new initialization method and dimensional winner-selection method, which was experimentally proven to results in better performance. We also reduced the size of feature vector without much degradation of performance.

Reference

[1] D. H. Zhang, Automated biometrics: Technologies and Systems, Kluwer Academic Publishers, 2000.

[2] F. H. Adler, *Physiology of the Eye: Clinical Application*, The C. V. Mosby Company, 1965.

[3] P. W. Hallinan, "Recognizing Human Eyes", SPIE Proc. of Geometric Methods in Computer Vision, Vol. 1570, pp. 214~226, 1991.

[4] John G. Daugman, "High Confidence Visual Recognition of Persons by a Test of Statistical Independence", IEEE Transaction on Pattern Analysis and Machine Intelligence, Vol. 15, No. 11, pp. 1148~1161, 1993.

[5] Richard P. Wildes, "Iris Recognition: An Emerging Biometric Technology", Proceedings of the IEEE, Vol. 85, No. 9, pp. 1348~1363, 1997.

[6] W. W. Boles and B. Boashash, "A Human Identification Technique Using images of the Iris and Wavelet Transform", IEEE Transaction on Signal Processing, Vol. 46, No. 4, pp. 1185~1188, 1998.

[7] D. de Martin-Roche, C. Sanchez-Avila, and R. Sanchez-Reillo, "Iris Recognition for Biometric Identifica-

tion using Dyadic Wavelet Transform Zero-Crossing," Security Technology, 2001 IEEE 35th International Carnahan Conference, pp. 272-277, 2001.

[8] Gerold O. Williams, "Iris Recognition Technology", IEEE AES Systems Magazine 1997, pp. 23~29, April 1997.

[9] W. K. Kong and D. Zhang, "Accurate iris segmentation based on novel reflection and eyelash detection model," Proceeding of 2001 International Symposium on Intelligent, Multimedia, Video and Speech Processing, May 2001, Hong Kong.

[10] M. Kass, A. Witkin, and D. Terzopoulos, "Sake: Active contour models," in Proceedings of First International Conference on Computer Vision, pp. 259-269, London, 1987.

[11] D. J. Williams and M. Shah, "A fast algorithm for active contours and curvature estimation," CVGIP: Image Understanding, Vol. 55, No. 1, January, pp.14-26, 1992.

[12] Gilbert Strang, Truong Nguyen, *Wavelets and Filter Banks*, Wellesley-Cambridge Press, 1996.

[13] L. Fausset, Fundamentals of Neural Networks, Prentice Hall, 1994.

[14] T. Kohonen, The *Self-organization and Associate Memory*, Springer-Verlag, 1985

[15] S. Cho and H. Seong, Iris recognition using Gabor transform and neural net , Journal of Fuzzy Logic and Intelligent Systems, Vol. 7, No. 2, pp. 397¡ 401, 1997.

Table 1. Parameter values for LVQ

Learning rate	0.1
Update of learning rate	
Total number of iteration	300

Table 2. Classification rates of two different feature extraction methods

	Gabor transform	Wavelet transform
Learning data	98%	98%
Test data	93%	94%

Table 3. Classification Rate of two different initialization methods

	Random initialization method	The proposed initialization method
Learning data	98%	100%
Test data	94%	98%

Table 4. Classification rates of a known winner-selection method using various distance measures

Norm	Classification rate	
1-norm	98%	$\lvert\cdot\rvert+\lvert\cdot\rvert+\cdots$
2-norm	98%	$\sqrt{\lvert\cdot\rvert^2+\lvert\cdot\rvert^2+\cdots}$
-norm	94%	$\max\{\lvert\cdot\rvert+\lvert\cdot\rvert+\cdots\}$

Table 5. Classification rates of two different winner-selection methods

	Winner-selection method using Euclidean distance	The proposed dimensional winner-selection method
Learnin	100%	100%
Test Data	98%	100%

Table 6. Classification Rate of feature vectors with different sizes

	93 dimensions (4 bytes / dimension)	87 dimensions (1 bit / dimension)
Learning data	100%	100%
Test data	100%	100%

Table 7. Classification Rates

Feature extraction method	Gabor transform	Wavelet transform			
Classification method	Random initialization		The proposed initialization method		
	Winner-selection method using Euclidean distance			The proposed dimensional winner-selection	
Data size	93 dimensions (4 bytes/dimension)				87 dimension (1 bit/dim.)
Learning data	98%	98%	100%	100%	100%
Test data	93%	94%	98%	100%	100%

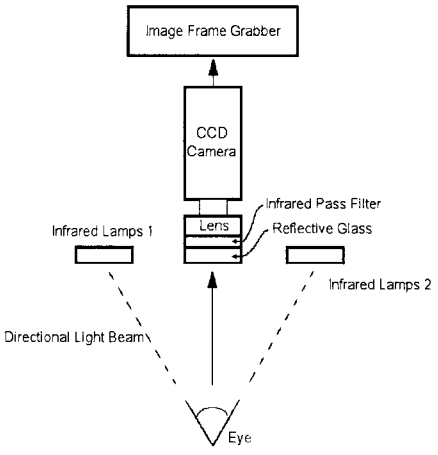

Fig. 1 The iris acquisition system viewed from the top. Two infrared lamps are placed at a higher position than the human eye.

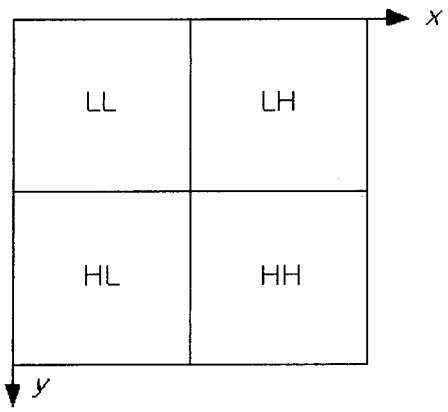

Fig. 2 Decomposition of 2D signal

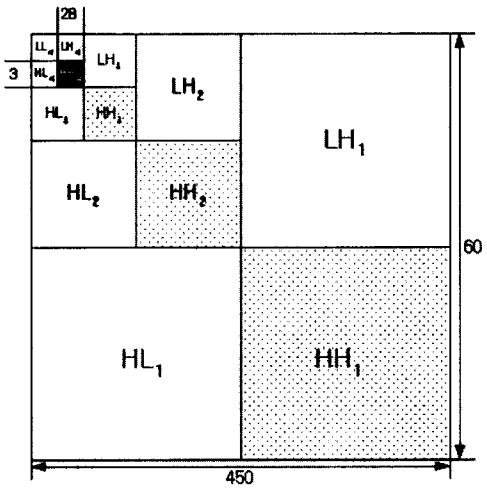

Fig. 3 Pyramid decomposition of the iris pattern

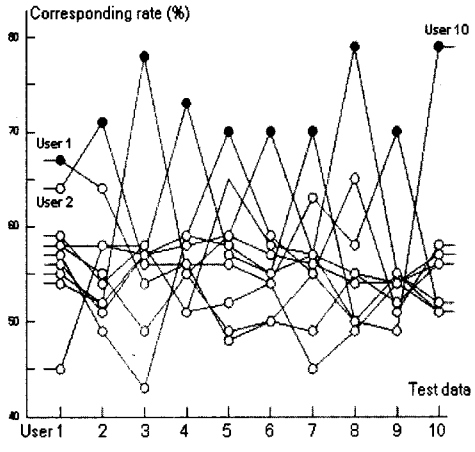

Fig. 4 The results using the feature vectors extracted HH4 obtained by 4 time decomposition.

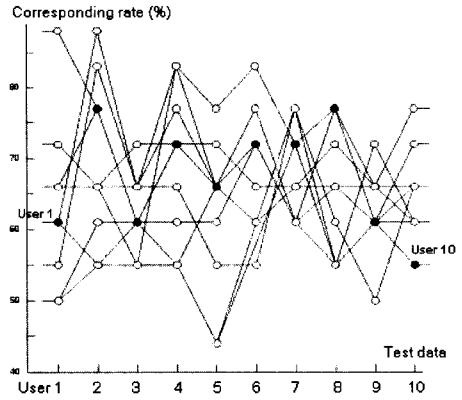

Fig. 5 The results using the feature vectors extracted HH4 obtained by 5 time decomposition.

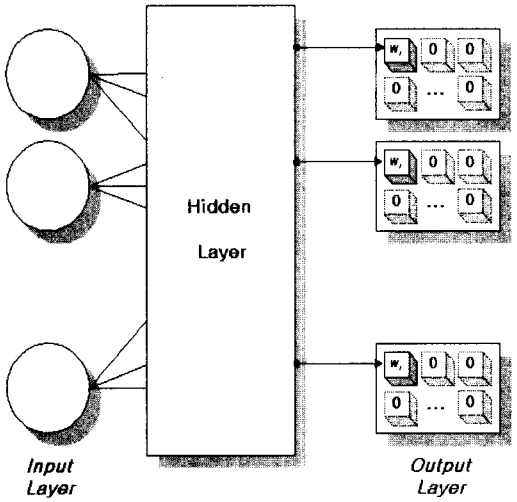

Fig. 6 The initialization of the weighting vectors [Step 1].

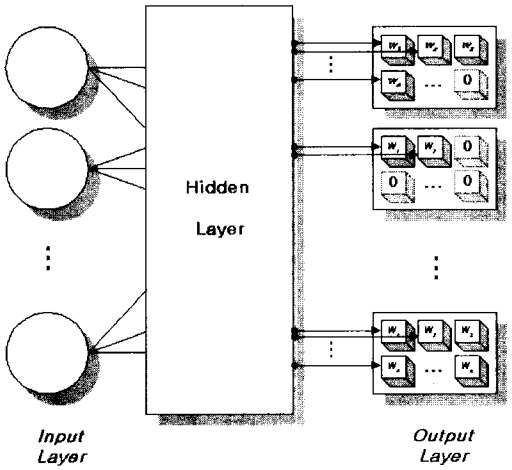

Fig. 7 The neural network after the initialization procedure

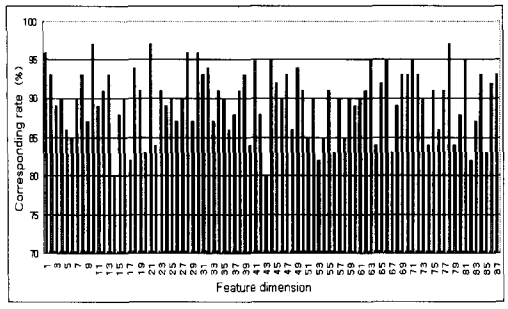

Fig. 8 Corresponding rate of each feature element

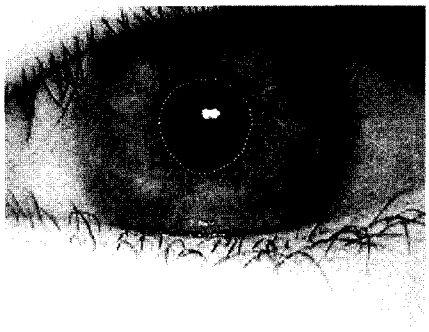

(a)

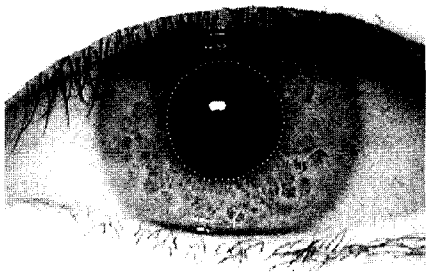

(b)

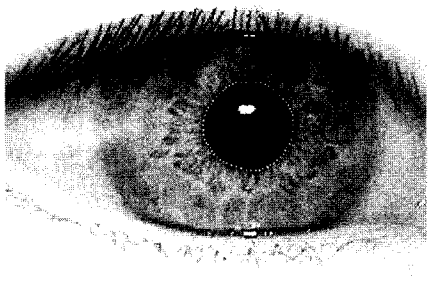

(c)

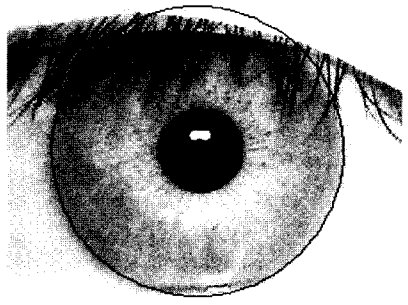

(d)

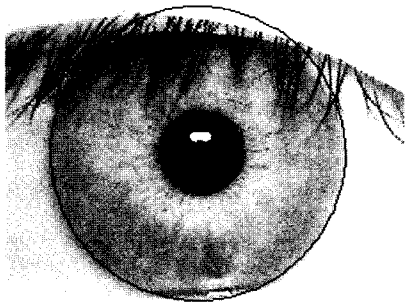

(e)

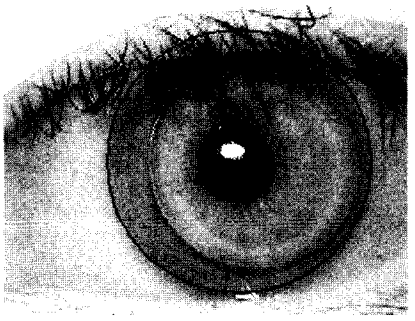

(f)

Fig. 9 The estimation results of pupillary boundaries and limbus

Soengwon Cho

He received the B.S. and M.S. degrees in electrical engineering from Seoul National University in 1982. He received the M.S. and Ph.D. degrees in electrical engineering from Purdue university in 1987 and 1992, respectively. He is with Hongik University as an associate professor at School of electronics and electrical engineering. His research interests are biometrics, artificial intelligence, and pattern recognition.

Phone : +82-2-320-1493

Fax : +82_2-320-1110

E-mail : swcho@hongik.ac.kr

Jaemin Kim
He received the B.S. and M.S. degrees in electrical engineering from Seoul National University in 1984 and 1986, respectively. He from Rensselaer Polytechnic Institute in 1994. He is with Hongik University as an assistant professor at School of electronics and electrical engineering. His research interests are biometrics, bioinfomatrics, image processing and compute vision.

Phone : +82-2-320-1634
Fax : +82_2-320-1110
E-mail : jaemin@hongik.ac.kr

Jungwoo Won
He received the B.S. degrees in electronics and electrical engineering from Hongik University in 2002.
In 2002-2003, He was a Research Assistant in the Hongik University Artificial Intelligence Laboratory. He is majoring Image Processing at graduate school of Hongik University. His research interests are biometrics, pattern recognition and image processing.

Phone : +82-2-320-1493
Fax : +82_2-320-1110
E-mail : chojjaya@empal.com